Transp Porous Med (2007) 70:279–292
DOI 10.1007/s11242-007-9099-2

ORIGINAL PAPER

A Lattice Boltzmann study of non-newtonian flow in digitally reconstructed porous domains

J. Psihogios · M. E. Kainourgiakis · A. G. Yiotis · A. Th. Papaioannou · A. K. Stubos

Received: 12 September 2006 / Accepted: 7 January 2007 / Published online: 5 May 2007

Abstract In the present study, the Lattice Boltzmann Method (LBM) is applied to simulate the flow of non-Newtonian shear-thinning fluids in three-dimensional digitally reconstructed porous domains. The non-Newtonian behavior is embedded in the LBM through a dynamical change of the local relaxation time. The relaxation time is related to the local shear rate in such a way that the power law rheology is recovered. The proposed LBM is applied to the study of power-law fluids in ordered sphere packings and stochastically reconstructed porous domains. A linear relation is found between the logarithm of the average velocity and the logarithm of the body force with a curve slope approximately equal to the inverse power-law index. The validity of the LBM for the flow of shear thinning fluids in porous media is also tested by comparing the average velocity with the well known semi-empirical Christopher–Middleman correlation. Good agreement is observed between the numerical results and the Christopher–Middleman correlation, indicating that the LBM combined with digital reconstruction constitutes a powerful tool for the study of non-Newtonian flow in porous media.

Keywords Non-Newtonian flow · Lattice-Boltzmann method · Stochastic reconstruction · Porous media permeability

1 Introduction

Transport in disordered media is a topic related to many technological and environmental applications. The accurate prediction of the transport coefficients in disordered

J. Psihogios · M. E. Kainourgiakis (✉) · A. G. Yiotis · A.K. Stubos
National Center of Scientific Research 'Demokritos', 15310, Ag. Paraskevi Attikis, Athens, Greece
e-mail: kainourg@ipta.demokritos.gr

J. Psihogios · A.Th. Papaioannou
National Technical University of Athens, Department of Chemical Engineering, Iroon Polytechneiou Str. 9, 15780, Athens, Greece

media is a challenging problem due to the complexity of transport mechanisms in fluid–solid systems and the difficulty in representing accurately the complicated and tortuous nature of a porous medium. The Lattice Boltzmann method (LBM) constitutes a very powerful tool for the study of the hydrodynamical problem of fluid flow inside porous structures, mainly due to the simplified handling of the complicate boundary conditions, as well as, due to the efficiency of the method with regard to parallelization (Succi 2001; Sukop and Thorne 2006).

Aharonov and Rothman (1993) first used the LB method to simulate the flow of non-Newtonian fluids. Their pioneering work addresses two dimensional pipes and random media. They found that the flux is related to the driving force by a simple scaling law. Similar results were reported by Boek et al. (2003). Recently, Gabbanelli et al. (2005) studied the flow of truncated power-law fluids in reentrant flow geometries and found a very good agreement between the results obtained by the LBM and those obtained by standard finite element methods, while Sullivan et al. (2006) explored the relationship between lattice resolution and simulation accuracy as a function of the power-law index.

In the present study the LBM is applied to simulate the flow behavior of non-Newtonian fluids in three-dimensional digitally reconstructed porous domains. The digital reconstruction of the porous matrix is achieved by the use of stochastic reconstruction, where the domain produced has the same statistical content with the actual material. The results indicate that the combination of the LB technique with digital reconstruction can be a very powerful tool for the study of those systems, which are of great interest for a variety of technological fields such as oil recovery and underground water contamination.

2 Lattice Boltzmann approach

2.1 General remarks

LBM is a numerical method for the solution of fluid mechanical problems especially in systems where the fluid–solid interface is very complex (Succi 2001). Space, time and momentum are discretized and the fluid behavior is described by the particle distribution function, f_i(**x**,t), which represents the number density of particles on node **x**, at time t, with velocity $\mathbf{e}_i$. The density $\rho(\mathbf{x}, t)$ and the velocity $\mathbf{u}(\mathbf{x}, t)$ are recovered by:

$$\rho(\mathbf{x}, t) = \sum_{i=0}^{q} f_i(\mathbf{x}, t) \tag{1}$$

$$\rho(\mathbf{x}, t)\mathbf{u}(\mathbf{x}, t) = \sum_{i=0}^{q} \mathbf{e}_i f_i(\mathbf{x}, t) \tag{2}$$

where, q is the number of the discrete directions of velocity (note that $i = 0$ corresponds to the 'rest particle'). In the present study the D3Q19 version is used, where D3 indicates three dimensions and Q19 nineteen velocity vectors (including the null vector). Denoting as δx the lattice spacing and as δt the time step, the corresponding nineteen discrete velocity vectors are defined as follows:

$$\mathbf{e}_i = \begin{cases} (0,0,0)c & & & i=0 \\ (\pm1,0,0)c & (0,\pm1,0)c & (0,0,\pm1)c & i=1,2,\ldots,6 \\ (\pm1,\pm1,0)c & (\pm1,0,\pm1)c & (0,\pm1,\pm1)c & i=7,8,\ldots,18 \end{cases} \tag{3}$$

where $c = \delta x/\delta t$

The space-time evolution of $f_i(\mathbf{x},t)$ is assumed to obey the equation:

$$f_i(\mathbf{x}+\mathbf{e}_i\delta t, t+\delta t) - f_i(\mathbf{x},t) = \Omega_i \tag{4}$$

where Ω_i, is the collision operator, which can be approximated as a constant rate, of the approach of $f_i(\mathbf{x},t)$ to an appropriately chosen equilibrium distribution, $f_i^{(eq)}(\mathbf{x},t)$ (Bhatnagar–Gross–Krook approximation). Thus:

$$\Omega_i = -\frac{1}{\tau_0}\left[f_i(\mathbf{x},t) - f_i^{(\mathrm{eq})}(\mathbf{x},t)\right] \tag{5}$$

where, τ_0, is the non-dimensional relaxation time associated with the kinematic viscosity, ν_0, of the fluid by the relation:

$$\nu_0 = c_s^2\delta t\,(\tau_0 - 0.5) \tag{6}$$

The parameter c_s corresponds to the lattice speed of sound. For the D3Q19 model $c_s/c = 1/\sqrt{3}$. Furthermore, the relaxation time may only take values $\tau_0 > 0.5$.

In order to recover isotropic hydrodynamic behavior the equilibrium distribution is chosen to be:

$$f_i^{(\mathrm{eq})}(\mathbf{x},t) = w_i\rho(\mathbf{x},t)\left[1 + \frac{\mathbf{e}_i\cdot\mathbf{u}(\mathbf{x},t)}{c_s^2} + \frac{(\mathbf{e}_i\cdot\mathbf{u}(\mathbf{x},t))^2}{2c_s^4} - \frac{\mathbf{u}(\mathbf{x},t)\cdot\mathbf{u}(\mathbf{x},t)}{2c_s^2}\right] \tag{7}$$

where, w_i is the appropriate weighting factor with values:

$$w_i = \begin{cases} 1/3 & i=0 \\ 1/18 & i=1,2,\ldots,6 \\ 1/36 & i=7,8,\ldots,18 \end{cases} \tag{8}$$

In the presence of a body force density $\mathbf{F} = \rho\mathbf{g}$, where $\mathbf{g}$ is the acceleration due to $\mathbf{F}$, Eq. (4) becomes:

$$f_i(\mathbf{x}+\mathbf{e}_i\delta t, t+\delta t) - f_i(\mathbf{x},t) = \Omega_i + \delta t\hat{F}_i(\mathbf{x},t) \tag{9}$$

where the momentum source term $\hat{F}_i(\mathbf{x},t)$ obeys the relation (Guo et al. 2002):

$$\hat{F}_i(\mathbf{x},t) = \left(1 - \frac{1}{2\tau_0}\right)w_i\left\{\frac{\mathbf{e}_i - \mathbf{u}(\mathbf{x},t)}{c_s^2} + \frac{[\mathbf{e}_i\cdot\mathbf{u}(\mathbf{x},t)]}{c_s^4}\mathbf{e}_i\right\}\cdot\mathbf{F} \tag{10}$$

The fluid density is still given by Eq. (1) while the fluid velocity satisfies:

$$\rho(\mathbf{x},t)\mathbf{u}(\mathbf{x},t) = \sum_{i=1}^{q}\mathbf{e}_i f_i(\mathbf{x},t) + \frac{\delta t}{2}\mathbf{F} \tag{11}$$

In the present study, no-slip boundary conditions were employed at the fluid-solid boundaries using the bounce-back convention. If the lattice node $\mathbf{x}$ is in the fluid and the adjacent node, $\mathbf{x} - \mathbf{e}_i\delta t$ is located inside the solid boundary, defining $\mathbf{e}_{i'} = -\mathbf{e}_i$, the distribution function at the next time step $f_i(\mathbf{x}, t+\delta t)$ is determined by (Maier et al. 1998; Aidun et al. 1998):

$$f_i(\mathbf{x}, t+\delta t) = f_{i'}(\mathbf{x},t) + \Omega_i + \delta t\hat{F}_i \tag{12}$$

The derivation of the macroscopic equations obeyed by Eqs. (1)–(12) is described in detail in Guo et al. (2002) and Zou and He (1999). Briefly, a Taylor expansion in time and space is performed and the long-wavelength and low-frequency limit of the lattice-Boltzmann equation for the single-particle distribution is taken. The result is a continuum form of the Boltzmann equation correct to second order in the lattice spacing and the time step. A scaling expansion argument and the neglect of higher-order terms lead to the following final form of the macroscopic equations obeyed by the simulated system:

$$\frac{\partial \rho}{\partial t} = \nabla \cdot \rho \mathbf{u} \tag{13}$$

$$\frac{\partial (\rho \mathbf{u})}{\partial t} + \nabla \cdot (\rho \mathbf{u}\mathbf{u}) = -\nabla p + \nu_0 \nabla \cdot \{\rho[\nabla \mathbf{u} + (\nabla \mathbf{u})^T]\} + \mathbf{F} \tag{14}$$

where, $p = c_s^2 \rho$.

2.2 Non-Newtonian behavior

For certain simple types of non-Newtonian fluids the relation between the shear stress, σ, and the rate of deformation tensor, $\dot{\gamma}(\mathbf{x})$, where:

$$\dot{\gamma}(\mathbf{x}) = \nabla \mathbf{u}(\mathbf{x}) + (\nabla \mathbf{u}(\mathbf{x}))^T \tag{15}$$

is described by:

$$\sigma = \mu(I_2)\dot{\gamma} \tag{16}$$

where $\mu(I_2)$ is the scalar non-Newtonian viscosity and I_2 the second invariant of the rate of deformation tensor, defined by: $I_2 = \dot{\gamma}(\mathbf{x}) : \dot{\gamma}(\mathbf{x})$.

The dependence of the non-Newtonian viscosity on I_2 can be implemented in LBM through the assumption that the constant relaxation time in Eq.(5) is replaced by the function $\tau(I_2)$ which obeys the relation:

$$\tau(I_2) = \frac{\nu(I_2)}{c_s^2 \delta t} + \frac{1}{2} \tag{17}$$

where $\nu(I_2) = \mu(I_2)/\rho$.

In the present study the shear thinning Ostwald—de Waale fluids are considered. For these fluids the apparent non-Newtonian viscosity $\mu(I_2)$ is taken to be a power-law function of I_2, specifically:

$$\mu(I_2) = \mu^* \left(\sqrt{\frac{1}{2} I_2} \right)^{n-1} \tag{18}$$

where μ^* is the consistency index and n is the flow-behavior exponent index. Note that for $n = 1$ the Newtonian behavior is recovered with viscosity $\mu = \mu^*$, for $n < 1$ the effective viscosity decreases with increasing shear stress (pseudoplastic or shear-thinning fluid), while, for $n > 1$ the viscosity increases with increasing shear stress (dilatant or shear-thickening fluid).

The consistency index can be linked with the relaxation time of the Newtonian fluid by a relation similar to Eq. (5), since it can be regarded as the viscosity of the fluid when $n = 1$:

$$\mu^* = (\tau_0 - 0.5)\delta t^n \rho\, c_s^2 \tag{19}$$

Combining Eqs. (17), (18), (19) the relaxation time becomes:

$$\tau(I_2) = \left(\tau_0 - \frac{1}{2}\right)\left(\delta t\sqrt{\frac{1}{2}I_2}\right)^{n-1} + \frac{1}{2} \tag{20}$$

3 Representation and characterization of the porous domains

3.1 General remarks

The spatial distribution of matter in a porous medium can be typically represented by the phase function $Z(\mathbf{x})$, defined as follows:

$$Z(\mathbf{x}) = \begin{cases} 1 & \text{if } \mathbf{x} \text{ belongs to pore space} \\ 0 & \text{otherwise} \end{cases} \tag{21}$$

where $\mathbf{x}$ is the position vector from an arbitrary origin. Due to the disordered nature of porous media, $Z(\mathbf{x})$ can be considered as a stochastic process, characterized by its statistical properties. The porosity, ε, and the auto-correlation function $R_Z(\mathbf{r})$ can be defined by the statistical averages (Adler 1992; Berryman 1985):

$$\varepsilon = \langle Z(\mathbf{x}) \rangle \tag{22}$$

$$R_Z(\mathbf{r}) = \frac{\langle (Z(\mathbf{x}) - \varepsilon) \cdot (Z(\mathbf{x}+\mathbf{r}) - \varepsilon) \rangle}{\varepsilon - \varepsilon^2} \tag{23}$$

Note that $\langle \cdot \rangle$ indicates spatial average. For an isotropic medium, $R_Z(\mathbf{r})$ becomes one-dimensional as it is only a function of $r = |\mathbf{r}|$ (Adler 1992; Berryman 1985).

3.2 Stochastic reconstruction

The purpose of the stochastic reconstruction procedure is the generation of a digitized three-dimensional snapshot of $Z(\mathbf{x})$ with the same statistical behavior as those measured on a single two-dimensional section of the material. The statistical content expressed properly by the various moments of the phase function. In practice, matching of the first-two moments, that is, porosity and auto-correlation function, has been customarily pursued, although this simplification is not generally valid as one can find examples of porous media exhibiting quite different morphological properties while sharing the same $R_Z(\mathbf{r})$ (Kainourgiakis et al. 2000; Roberts 1997; Talukdar 2002). In this case one should try to match multi-point correlation functions (Yeong and Torquato 1998).

The reconstructed porous domains are generated by the convolution of a random and spatially uncorrelated field with a kernel, which contains information about the actual porous structure. The space is discretized in N^3 cubic elements, the position of which is characterized by the vector $\mathbf{x} = (i, j, k)$ where i, j, k integers with values $1, 2, \ldots, N$ and a random spatially uncorrelated value $X(\mathbf{x})$ is assigned to any element. A smooth, spatially correlated field $Y(\mathbf{x})$ with a correlation function $R_Y(\mathbf{r})$, can be

deduced from the $X(\mathbf{x})$ field by the convolution:

$$Y(i,j,k) = \sum_{k'=-\infty}^{+\infty} \sum_{j'=-\infty}^{+\infty} \sum_{i'=-\infty}^{+\infty} R_Y(i-i', j-j', k-k') X(i', j', k') \tag{24}$$

where, $\mathbf{r} = (i-i', j-j', k-k')$.

The correlated field $Y(\mathbf{x})$ is then binarized in order to produce the target phase function $Z(\mathbf{x})$ (i.e., the stochastically reconstructed sample). In general the discretization occurs through a thresholding procedure:

$$Z(\mathbf{x}) = \begin{cases} 1 & \text{if } Y(\mathbf{x}) < Y_0 \\ 0 & \text{elswhere} \end{cases} \tag{25}$$

where Y_0 is chosen in such a way that Eq. (23) is satisfied.

The correlation function $R_Y(\mathbf{r})$ can be deduced by observation, as in Crossley et al. (1991) or by a standard procedure which is described in detail in Adler (1992). According to the latter approach the kernel of a stationary and isotropic medium is computed from the autocorrelation function $R_Z(\mathbf{r})$ that is obtained directly by microscopy or indirectly by small angle scattering techniques, by:

$$R_Z(r) = \sum_{m=0}^{\infty} c_m^2 R_Y^m(r) \tag{26}$$

The coefficients c_m are given by

$$c_m = (2\pi m)^{1/2} \int_{-\infty}^{+\infty} C(y) \exp(-y^2/2) H_m(y) \mathrm{d}y \tag{27}$$

where $H_m(y)$ is the Hermite polynomial of mth order:

$$H_m(y) = (-1)^m \exp(y^2/2) \frac{\mathrm{d}^m}{\mathrm{d}y^m} \exp(-y^2/2) \tag{28}$$

and

$$C(y) = \begin{cases} \dfrac{\varepsilon - 1}{\left[\varepsilon(1-\varepsilon)\right]^{1/2}} & \text{if } P(y) \le \varepsilon \\ \dfrac{\varepsilon}{\left[\varepsilon(1-\varepsilon)\right]^{1/2}} & \text{if } P(y) > \varepsilon \end{cases} \tag{29}$$

with

$$P(y) = (2\pi)^{1/2} \int_{-\infty}^{y} \exp(-t^2/2) \mathrm{d}t \tag{30}$$

Furthermore the initial field $X(\mathbf{x})$ corresponds to random values obeying normal distribution with zero mean and unit variance, a property that is inherited to $Y(\mathbf{x})$. Therefore the extraction of the binary phase function $Z(\mathbf{x})$ from the real array Y can be accomplished by the condition:

$$Z(\mathbf{x}) = \begin{cases} 1 & \text{if } P[Y(\mathbf{x})] \le \varepsilon \\ 0 & \text{otherwise} \end{cases} \tag{31}$$

which is equivalent with Eq. (25).

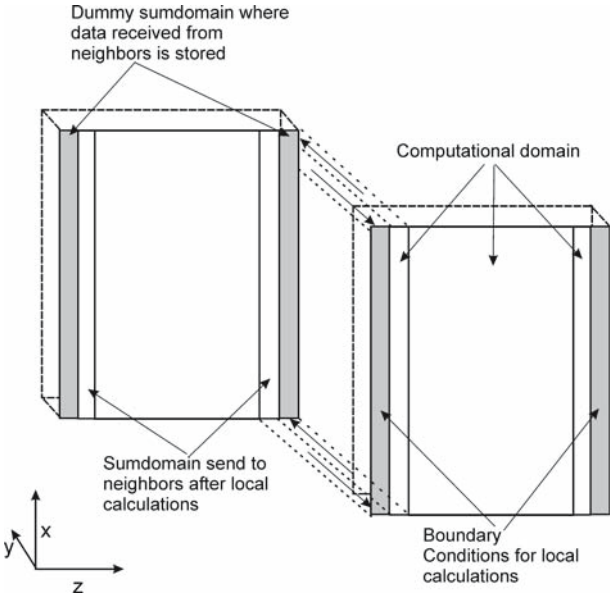

Fig. 1 Schematic of domain decomposition in our algorithm. The computational domain for each processor is shown in white color. At the boundaries of the computational subdomains the data calculated at the previous time step is stored in dummy subdomains (where no calculations take place) shown in gray color. The dummy subdomains serve as boundary conditions for the local calculations at the current time step. The computational domain (three-dimensional arrays) is decomposed in the z-direction in order to take advantage of Fortran's column-major storage of multi-dimensional array elements

4 Results and discussion

4.1 General remarks

The Lattice Boltzmann model described in the previous sections is parallelized for implementation on distributed memory computers using the Message Passing Interface (MPI) libraries. The computational domain (three-dimensional arrays) is decomposed in the z-direction in order to take advantage of Fortran's column-major storage of multi-dimensional array elements. This scheme ensures that array elements exchanged across processors with MPI are located in continuous memory blocks (Fig. 1).

The numerical simulations were performed on a cluster with 4 Intel Xeon processors (two dual-processor blades) operating at 3.6 GHz. The total memory of the blades is 4 GB (2 GB per blade). The blades are interconnected through a Gigabit Ethernet Network. The computer cluster is operated using the Clustermatic 5 set of software tools developed at Cluster Research Lab of the Los Alamos National Laboratory www.clustermatic.org. Our typical production runs were performed on all 4 CPUs using a total of 8 code threads in order to take advantage of the Hyper-Threading capabilities of the Xeon processors. A steady state velocity profile was reached in less than 10^5 time-steps (approximately 38 hours on 4 CPUs or 152 CPU-hours per simulation for the 160^3 lattice).

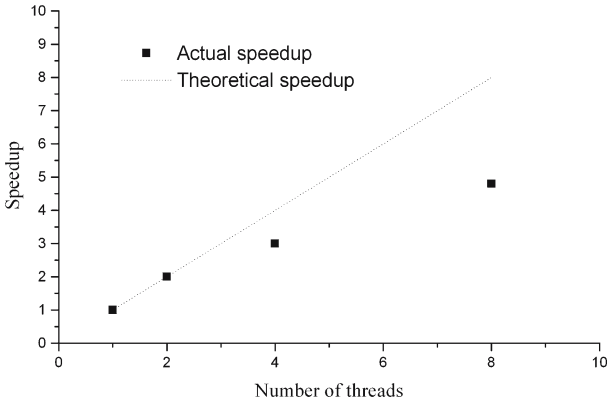

Fig. 2 Parallel speedup of the LB algorithm used in the present study

Table 1 Maximum velocity for the flow of power law fluids between parallel plates ($W = 48\delta x, \mu^* = 0.0067\delta t^n \rho\, c^2, |\mathbf{F}| = 10^{-9}\rho\delta x/\delta t^2$)

Power law index (n)	Maximum velocity Eq. (32)	Maximum velocity LBM
0.6	$7.61 \times 10^{-9}\ c$	$7.48 \times 10^{-9}\ c$
1	$4.32 \times 10^{-5}\ c$	$4.25 \times 10^{-5}\ c$

The parallel speedup of our algorithm is shown in Fig. 2. The speedup is defined as $S(p) = \frac{t(\text{serial})}{t(p)}$, where t(serial) is the execution time of the serial code and $t(p)$ is the execution time of the parallel code on p code threads (distributed evenly on the available system CPU's). The parallel efficiency E of our LB code is 0.74 for 4 code threads (on 4 CPUs) and drops to 0.61 for 8 code threads (on 4 CPU's). The parallel efficiency is defined as $E(p) = \frac{S(p)}{p}$.

4.2 Flow between parallel planes

In order to validate the LB procedure, the flow of power-law fluids between two parallel planes is considered first. The velocity profile of power-law fluids in such a case is described by:

$$u(y) = u_0 \left[1 - \left(\frac{2|y|}{W} \right)^{1+\frac{1}{n}} \right] \tag{32}$$

where

$$u_0 = \left(\frac{1}{\mu^*} |F| \right)^{1/n} \left(\frac{W}{2} \right)^{\left(1+\frac{1}{n}\right)} \left(\frac{n}{n+1} \right) \tag{33}$$

and W is the distance between the parallel plates.

The maximum velocity for each exponent ($n = 0.6, 1$) is shown in Table 1 while the velocity profile is illustrated in Fig. 3.

Very good agreement with the analytical solution is shown. The body force (and therefore the pressure gradient) is parallel to the plates, with magnitude $|\mathbf{F}| = 10^{-9}\rho\frac{\delta x}{\delta t^2}$. The relaxation time is equal to 0.52 (and therefore, according to

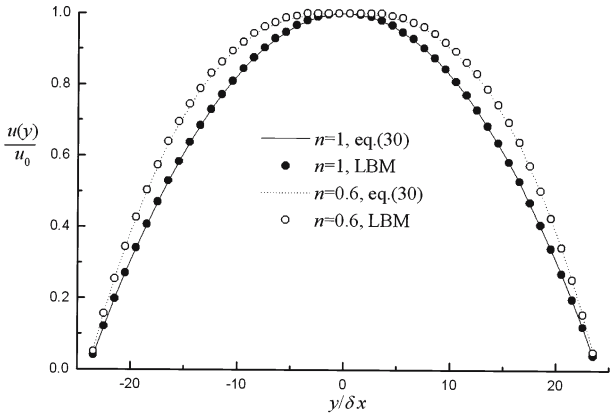

Fig. 3 The velocity profile obtained in a slit for a Newtonian and for a shear thinning fluid

Eq. (6), $\mu^* = 0.0067\delta t^n \rho\, c^2$) and the distance between the parallel plates $W = 48\delta x$. The density of the fluid is spatially and temporally uniform (incompressible flow).

4.3 Flow in arrays of spheres

The flow of a power-law fluid in an ordered (simple cubic) array of spheres is then examined. In a cubic packing, the spheres are stacked directly next to and on top of each other. The porosity of such a structure is $1 - \pi/6$. Due to the periodicity of the structure, the flow problem is solved in a very detailed unit cell of size 160^3 that contains only one sphere, illustrated in Fig. 4. The radius of the sphere is $R = 80\delta x$. Four exponents that indicate the power-law behavior of shear-thinning fluids have been considered, namely $n = 0.5, 0.7, 0.8, 1$. The applied body force is initially parallel to one of the principal axes of the domain and the resulting superficial velocity $< \mathbf{u} >$ is parallel to the body force due to the symmetry of the structure. The magnitude of the superficial velocity is plotted against the body force and the results are presented in Fig. 5. It is observed that the well-known scaling relation (Aharonov and Rothman 1993; Boek 2003; Sullivan et al. 2006; Shah and Yortsos 1995):

$$|\langle \mathbf{u} \rangle| \;\propto\; |\mathbf{F}|^{1/n} \tag{34}$$

is satisfied.

However, this result indicates only that the LB approach can reproduce qualitatively the fluid behavior and does not offer any information about the absolute value of the velocity profile. In this work an additional comparison is made in order to examine the quantitative accuracy of the technique in porous domains. The numerical results are compared with the semi-empirical equation proposed by Christofer and Middleman (1965) for the flow of non-Newtonian fluids in porous media.

For Newtonian fluids, the permeability tensor, $\boldsymbol{K}$, is defined by the Darcy equation:

$$\langle \mathbf{u} \rangle = -\frac{1}{\mu} \boldsymbol{K} \cdot \mathbf{F} \tag{35}$$

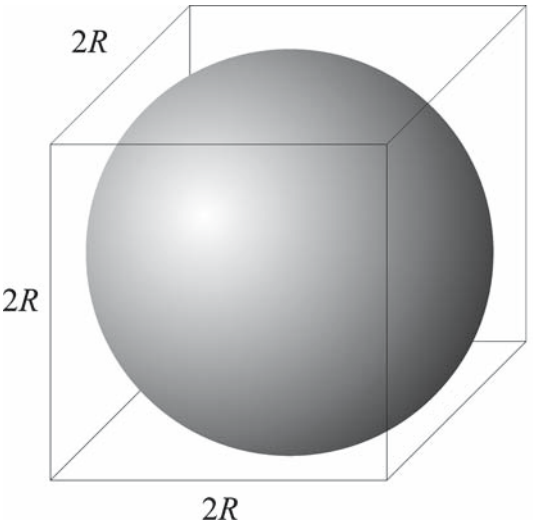

Fig. 4 The unit cell of an ordered (simple cubic) packing of spheres

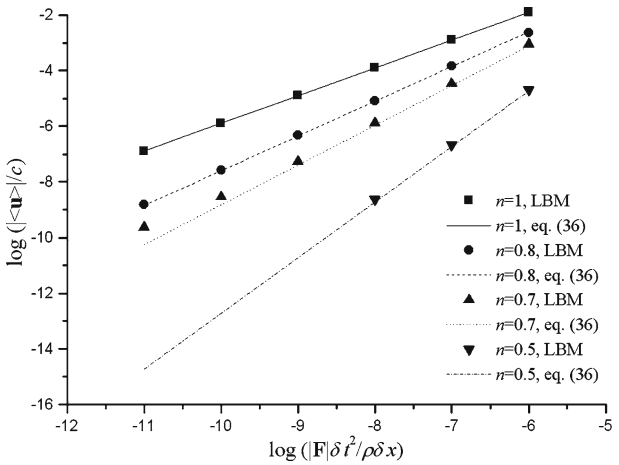

Fig. 5 The superficial velocity of Newtonian and shear-thinning fluids in a cubic packing of spheres. The consistency index is $\mu^* = 0.0067\delta t^n \rho\, c^2$

Since the sphere pack domain exhibits cubic symmetry, the permeability tensor can be expressed as:

$$\boldsymbol{K} = k\boldsymbol{I} \tag{36}$$

where, k is the permeability coefficient and $\boldsymbol{I}$ the unit tensor. Therefore Eq. (35) is reduced to:

$$\langle \mathbf{u} \rangle = -\frac{1}{\mu} k \cdot \mathbf{F} \tag{37}$$

For the Newtonian case, the permeability coefficient of the sphere packing can be calculated from Fig. 5. The relaxation time is $\tau_0 = 0.52$ resulting to a viscosity with value $\mu = 0.0067\delta t \rho\, c^2$. Thus, the permeability coefficient is $k = 85\delta x^2$.

According to Christofer and Middleman (1965), the superficial velocity of power-law fluids in porous domains obeys the equation:

$$|\langle \mathbf{u} \rangle| = \left(\frac{k}{H} |\mathbf{F}| \right)^{1/n} \tag{38}$$

where, H is the bed factor defined by:

$$H = \frac{\mu^*}{12} \left(9 + \frac{3}{n} \right)^n (150 k\varepsilon)^{(1-n)/2} \tag{39}$$

Teeuw and Hessekink (Shah and Yortsos 1995) proposed a different expression for the bed factor:

$$H = 2\mu^* k^{(1-n)/2} \left(\frac{3n+1}{\varepsilon n} \right)^n \left(\frac{\varepsilon}{8} \right)^{(1+n)/2} \tag{40}$$

which gives similar results with those obtained by Eq. (39). Thus for the rest of the paper the bed factor is evaluated using Eq. (39).

The superficial velocities obtained by the LB technique as well as those calculated by Eq. (38) for exponents spanning from $n = 0.5$ to $n = 1$ are presented in Fig. 5. A very good agreement is observed for $n > 0.5$, while for $n = 0.5$ the numerical results begin to deviate from the empirical expression at relatively low body forces where the shear rate tends to zero and therefore the viscosity tends to infinity. A similar behavior is reported in (Sullivan 2006). It can be deduced that for porous media represented by high-resolution binary domains, the LB technique produces relatively accurate results. Lower values of the exponent n have also been used but the accuracy of the results suddenly begins to fall and for very small exponents ($n \leq 0.3$) the technique does not converge. The use of the relaxation parameter described by Sullivan in order to smooth the viscosity field during the simulation does not change the overall behavior. Furthermore, no truncation of the viscosity is performed in order to have a system that directly corresponds to Eq.(38).

The anisotropy that the non-Newtonian flow exhibits in certain structures (Idris 2004) is also examined. Initially the flow of a Newtonian and a non-Newtonian fluid in a square array of cylinders similar to the one used in (Idris 2004) is simulated. The porosity of the structure is 0.5 and the principal axis of each cylinder is parallel to the z-direction. The power-law exponents used are 1 and 0.5. If the applied body force is set parallel to x- or y-direction, the average velocity is also parallel to the body force. On the other hand, when the body force is not parallel to x- or y-direction and $n = 0.5$, the average velocity deviates slightly from the direction of the body force. The angle, β, between them can be determined by:

$$\beta = \arccos \frac{\langle \mathbf{u} \rangle \cdot \mathbf{F}}{|\langle \mathbf{u} \rangle| \, |\mathbf{F}|} \tag{41}$$

Specifically, if $\mathbf{F} = \left(\frac{1}{2}\mathbf{e}_x + \frac{\sqrt{3}}{2}\mathbf{e}_y + 0\mathbf{e}_z \right) 10^{-10} \frac{\rho \delta x}{\delta t^2}$ (where $\mathbf{e}_x$, $\mathbf{e}_y$, $\mathbf{e}_z$ is the basis of the 3D system of coordinates) then $\beta = 0$ is found for the Newtonian fluid, while for $n = 0.5$ a value of $\beta \approx 0.06$ rad is observed, in agreement with (Idris 2004).

Next, the cubic sphere pack is considered. The body force is set equal to $\mathbf{F} = \left(\frac{1}{\sqrt{14}}\mathbf{e}_x + \frac{2}{\sqrt{14}}\mathbf{e}_y + \frac{3}{\sqrt{14}}\mathbf{e}_z \right) 10^{-8} \frac{\rho \delta x}{\delta t^2}$. The angle between the velocity and the applied body force is found $\beta \approx 0.076$ rad, indicating that the slight anisotropy observed in the pseudo-3D square array of cylinders is also present in the sphere pack.

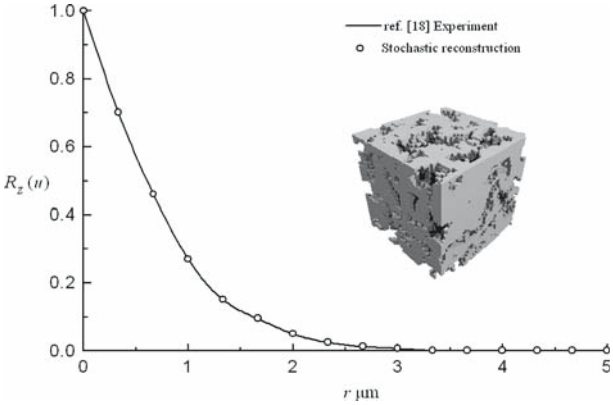

Fig. 6 Autocorrelation function and three-dimensional image of a digital domain obtained by stochastic reconstruction of North Sea chalk. The domain has porosity equal to 0.383, pixel length 0.2 μm, and size 160^3

4.4 Flow in stochastically reconstructed media

The usefulness of the LB technique for the study of the flow of shear-thinning fluids in porous media is further examined considering an amorphous reconstructed solid. In the previous section the porous material is crystalline (in the sense that it can be produced by the repetition of a certain unit cell) and therefore symmetric. Additionally, as a consequence of the crystallinity, a detailed solution can be achieved since a well-discretized unit cell (160^3) can be representative of the whole structure. In this section, we consider disordered but isotropic domain. This domain corresponds to a piece of North Sea chalk and it is produced by digital reconstruction as described above. The two-point autocorrelation function that is required as input for the stochastic reconstruction algorithm is taken from (Bekri 2000). The resulting domains are periodic and have porosity equal to 0.383, pixel length 0.2 μm, and size 160^3. In Fig. 6 a snapshot of the stochastically reconstructed sample and the corresponding autocorrelation functions are presented. The matching of the autocorrelation functions indicates that the reconstructed domain and the actual one exhibit disorder with similar statistical content in terms of the first two moments of the phase function.

The superficial velocity for different values of the power-law index (0.8, 1.0) and the pressure gradient is determined and the results are presented in Fig. 7. The consistency index is $\mu^* = 0.0067\delta t'' \rho\, c^2$. Since the binary domain is isotropic by construction, the permeability tensor can be again described by the permeability coefficient, which is determined for the Newtonian case ($n = 1$) by linear regression it is found to be $k = 0.12\delta x^2$. Recalling that for the reconstructed domain the pixel length is $\delta x = 0.2\mu$m, we conclude that $k = 4.8 \times 10^{-15}\text{m}^2$, in very reasonable agreement with the experimental value reported in (Bekri 2000).

In Fig. 7 the superficial velocity predicted by the correlation (38) is also presented and a satisfactory agreement with that obtained by the LB method is observed. Again the accuracy of the numerical results depends on the power-law index, small values of which induce negligible share rate and therefore extreme viscosity. Additionally the coarser discretization of the chalk domain compared to that of the sphere packing results to difficulties in convergence. Thus, if the objective is the detailed velocity

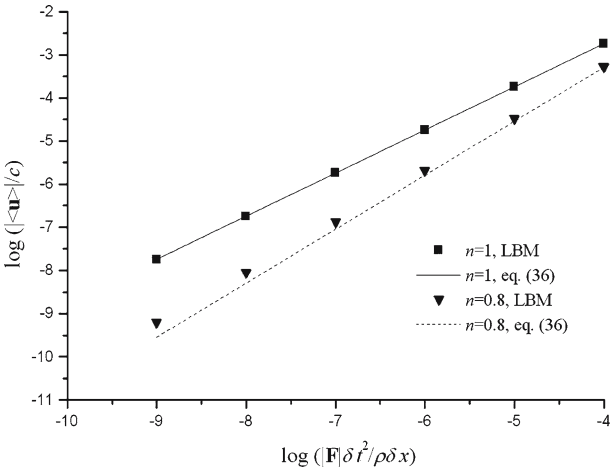

Fig. 7 The superficial velocity of a Newtonian and a shear thinning fluid in the digital domain obtained by stochastic reconstruction of North Sea chalk. The consistency index is $\mu^* = 0.0067\delta t^n \rho\, c^2$

field of a power-law fluid in the porous structure a high degree of discretization for the representation of the porous domain is required and therefore the corresponding computational resources are significant.

On the other hand, since Eq. (38) is valid (at least for power law indexes that are not very low) the information contained in the permeability coefficient regarding the geometry of the porous domain is sufficient to predict the average flow of a power-law fluid. Thus, the superficial velocity of a power law fluid in a reconstructed domain can be approximately evaluated using the data obtained from the Newtonian case. This renders the combination of the digital reconstruction with the determination of the Darcy permeability a powerful tool for the study of the non-Newtonian (power law) behavior in disordered porous solids.

5 Conclusions

In the present article the flow of shear-thinning fluids in porous media is investigated. Digitally reconstructed porous domains are considered, providing a detailed description of the actual pore space morphology. The velocity field of the fluid is determined by the application of LBM, where the non-Newtonian behavior is recovered by the appropriate dynamical change of the local relaxation time, which is considered as function of the local shear rate. It is found that not only the standard scaling relation between the average velocity and the overall force acting on the fluid is satisfied but also the actual value of the superficial velocity satisfies well-known semiempirical correlations (38) combined with (39) or (40). Furthermore, since LBM is accurate enough for the Newtonian case, the superficial velocity of a shear-thinning fluid in a reconstructed domain can be estimated by the Darcy permeability (obtained by LBM) combined with standard semiempirical correlations. Finally in the sphere pack domain it is found that the direction of the average velocity deviates slightly from the

direction of the body force when the body force is not parallel to one of the principal axes of the structure.

Acknowledgements We gratefully acknowledge the assistance of Mr Y. Xintavelonis to the setup of the computer infrastructure and the partial support by the European Commission (Contract EKN6-CT-2002-00602, ENVITRACER).

References

Adler, P.M.: Porous Media: Geometry and Transports. Butterworth, London (1992)
Aharonov, E., Rothman, D.H.: Non-Newotonian flow (through Porous media): a lattice Boltzmann method. Geophys. Res. Lett. **20**, 679–682 (1993)
Aidun, C.K., Lu, Y., Ding, A.-J.: Direct analysis of particulate suspensions with inertia using the discrete Boltzmann equation. J. Fluid Mech. **373**, 287–311 (1998)
Bekri, S., Xu, K., Yousefian, F., Adler, P.M., Thovert, J.-F., Muller, J., Iden, K., Psyllos, A., Stubos, A.K., Ioannidis, M.A.: Pore geometry and transport properties in North Sea chalk. J. Petroleum Sci. Eng. **25**, 107–134 (2000)
Berryman, J.G.: Measurement of spatial correlation functions using image processing techniques. J. Appl. Phys. **57**, 2374–2384 (1985)
Boek, E.S., Chin, J., Coveney, P.V.: Lattice Boltzmann Simulation of the flow of Non-Newtonian fluids in Porous Media. Int. J. Mod. Phys. B **17**, 99–102 (2003)
Christopher, R.H., Middleman S. Power law flow through packed tube. Ind. Eng. Chem. Fund. **4**, 422-(1965)
Crossley, P.A., Schwartz, L.M., Banavar, J.R.: Image-based models of porous media-Application to Vycor glass and carbonate rocks. Appl. Phys. Lett. **59**, 3553–3555 (1991)
Gabbanelli S., Drazer G., Koplik J. Lattice Boltzmann method for non-Newtonian (power-law) fluids. Phys. Rev. E **72**, 046312 (2005)
Guo Z., Zheng C., Shi B. Discrete lattice effects on the forcing term in the lattice Boltzmann method. Phys. Rev. E **65**, 046308 (2002)
http://www.clustermatic.org
Idris, Z., Orgéas, L., Geindreau, C., Bloch, J.-F., Auriault, J.-L.: Microstructural effects on the flow law of power-law fluids through fibrous media. Model. Simul. Mater. Sci. Eng. **12**, 995–1015 (2004)
Kainourgiakis, M.E., Kikkinides, E.S., Steriotis, T.A., Stubos, A.K., Tzevelekos, K.P., Kanellopoulos, N.K.: Structural and transport properties of alumina porous membranes from process-based and statistical reconstruction techniques. J. Colloid Interface Sci. **23**, 158–167 (2000)
Maier, R.S., Kroll, D.M., Kutsovsky, Y.E., Davis, H.T., Bernard, R.S.: Simulation of flow through bead packs using the lattice Boltzmann method. Phys. Fluids **10**, 60–74 (1998)
Roberts, A.P.: Statistical reconstruction of three-dimensional porous media from two-dimensional images. Phys. Rev. E **56**, 3203–3212 (1997)
Shah, C.B., Yortsos, Y.C.: Aspects of flow of power law fluids in porous media. AIChE J. **41**, 1099–1111 (1995)
Succi, S.: The Lattice Boltzmann Equation For Fluid Dynamics and Beyond. Oxford University Press, Oxford (2001)
Sukop, M.C., Thorne, Jr. D.T.: Lattice Boltzmann Modeling. An Introduction for Geoscientists and Engineers. Springer (2006)
Sullivan, S.P., Gladden, L.F., Johns, M.L.: Simulation of power-law fluid flow through porous media using lattice Boltzmann techniques. J. Non-Newtonian Fluid Mech. **133**, 91–98 (2006)
Talukdar, M.S., Torsaeter, O., Ioannidis, M.A.: Stochastic reconstruction of particulate media from two-dimensional images. J. Colloid Interface Sci. **248**, 419–428 (2002)
Yeong, C.L.Y., Torquato, S.: Reconstructing random media. II. Three-dimensional media from two-dimensiomal cuts. Phys. Rev. E **58**, 224–233 (1998)
Zou, Q., He, X.: Derivation of the macroscopic continuum equations for multiphase flow. Phys. Rev. E **59**, 1253–1255 (1999)